2023 62nd IEEE Conference on Decision and Control (CDC)
December 13-15, 2023. Marina Bay Sands, Singapore

Distributed Multi-robot Flocking based on Acoustic Doppler Effect

Yizhi Zhou, Cameron Nowzari and Xuan Wang

Abstract— **This paper aims to design a distributed algorithm based on Doppler effect that allows multiple robots to achieve a consensus on their velocities. Instead of relying on a direct measurement of robots' exact or relative velocities, which are usually challenging under denied environments (i.e., underwater), the novelty of our approach stems from utilizing the sound frequency as a medium to coordinate velocities among robots. Such a mechanism is achieved by exploiting the Doppler effect and establishing an equivalence between the velocity consensus of the robots and the frequency consensus of the sound they broadcast/receive. To address scalability and interference issues for large-scale systems, our use of the Doppler effect is broadcast-based, unlike most traditional Doppler devices that are reflection-based. Building on this, we develop a fully distributed algorithm for multi-robot flocking for the one-dimensional case, where the only control input for each robot is the sound frequencies it locally receives. The designed controller leads to highly nonlinear system dynamics. We employ a linearization method to theoretically prove the local convergence of the system to the desired equilibrium for velocity consensus. Simulations demonstrate the effectiveness of the proposed approach.**

I. Introduction

In recent years, distributed control of multi-agent systems has attracted increasing attention for its potential and various applications in mobile robots [1], sensor networks [2], [3], spacecraft systems [4], and so on. Compared with conventional centralized control schemes, distributed algorithms are more suitable for coordinating large-scale systems, due to their significant benefits in scalability, efficiency [5], [6] and robustness [7], [8]. Among the wide range of applications where distributed algorithms have been developed, one key problem is state consensus [9], which enables all the agents to asymptotically agree upon a common value through local information exchange and computation. In the existing literature, most distributed consensus algorithms rely on direct measurements of robots' states. However, in certain environments (underwater, indoor, etc.), obtaining such measurements is challenging owing to the limitations of communication and perception [10]. Motivated by this, we propose an alternative approach for multi-robot systems to achieve velocity consensus based on the Doppler effect. The approach is fully distributed and only relies on the broadcasted and received sound frequencies by robots.

Literature review: A large body of research on distributed flocking control of multi-agent systems has been established in the past years [11], [12]. The goal is to control the velocities of the robots, through local coordination, to achieve a synchronized quantity. Towards this end, algorithms have been developed based on a consensus mechanism, the key idea of which is to let each robot repeatedly update its own velocity towards the average of its neighbor's velocities. If the communication topology of the robot is spanned by a rooted directed tree, it is guaranteed that the velocities converge asymptotically [5], [13]. Besides, in the case that exact velocity cannot be measured, the robots can also make use of their relative velocities, then collectively drive such difference to zero [14].

While distributed consensus provides an elegant approach for solving flocking control of large-scale mobile robots, it requires robots to take direct/relative measurements of their states then share such information through local communication. However, such a requirement faces challenges under denied environments, e.g., underwater, high-rise buildings, indoor scenarios, when stable inter-robot communication and state measurement are mostly prohibited. Many existing communication approaches are not directly applicable for denied environments. For instance, optical communication can be used for high bandwidth and secure data transmission [15], but their performance can be easily affected by obstacles such as suspended particles in the water [16]. Electrocommunication is not efficient underwater due to high attenuation [17]. Acoustic communication is a commonly used method [18] in the environments where wireless communications are denied, because sound can travel through obstacles or penetrate water more easily than electromagnetic waves. However, traditional acoustic-based approaches are limited by their narrow bandwidth for data transmission and poor signal-to-noise ratio (SNR) tolerance [19]. For state measurement, we consider environments that GPS are denial. The robots then cannot accurately acquire their positions and velocities due to the lack of ways to eliminate the cumulative error on IMUs [20]. When using relative position/velocity to control the robots, radars and optical localization methods are prohibited. One may use sonars for underwater localization, but they suffer from slow response time and their mechanism based on sound reflection can cause strong interference when the number of robots grows large [21].

Statement of Contributions: This paper describes a novel approach for multi-robot flocking (velocity consensus) by exploiting a broadcast-based Doppler effect. We first formulate a multi-robot flocking control problem by assuming the robots cannot measure their velocities, but can only broadcast a sound at a certain frequency and receive the sound broadcasted by others. Then, through the Doppler effect, we establish an equivalence between sound frequency consensus and velocity consensus. Such a mechanism also distinguishes the proposed broadcast-based Doppler effect with traditional Doppler applications that relies on sound

Y. Zhou, C. Nowzari and X. Wang are with the Department of Electrical and Computer Engineering, George Mason University, Fairfax. Point of contact: xwang64@gmu.edu. Partial support of this research was provided by the Woodrow W. Everett, Jr. SCEEE Development Fund in cooperation with the Southeastern Association of Electrical Engineering Department Heads.

reflection. Building on the equivalence, we propose a fully distributed control algorithm for one-dimensional case where the robots adjust their velocity and achieve consensus solely based on the sound they broadcast/receive. The developed system dynamics are highly nonlinear, and we theoretically prove its local stability. The effectiveness of the proposed approach is verified by simulations.

Notation: Let $\mathbb{R}$, $\mathbb{C}$ denote the sets of real and complex numbers; $\mathbb{R}_+$ denote the set of positive real numbers. Let $\mathbf{1}_r$ denote the vector in $\mathbb{R}^r$ with all entries equal to 1. Let I_r denote the $r \times r$ identity matrix. We let $\text{col}\{A_1, A_2, \cdots, A_r\} = \begin{bmatrix} A_1^\top & A_2^\top & \cdots & A_r^\top \end{bmatrix}^\top$ be a vertical stack of matrices $A_1, \cdots, A_r$ possessing the same number of columns. Let $\text{diag}\{A_1, A_2, \cdots, A_r\}$ be a diagonal stack of matrices $A_1, \cdots, A_r$. Let $\boldsymbol{x}[i] \in \mathbb{R}$ be the ith entry of vector $\boldsymbol{x}$; correspondingly, let $M[i,j] \in \mathbb{R}$ be the entry of matrix M on its ith row and jth column. We denote by $M^\top$ the transpose of M.

II. Multi-robot Flocking based on Acoustic Doppler's Effect

Consider a network of m mobile robots where each robot i moves at a velocity $v_i \in \mathbb{R}^3$. The goal of multi-robot flocking control is to achieve a consensus on the velocities of all robots, such that

$$v^\star = v_1^\star = v_2^\star = \cdots = v_m^\star. \tag{1}$$

If the velocities of the robots can be measured and exchanged among robots, efficient distributed algorithms have been developed to achieve the consensus in (1) [11]. However, in this paper, we assume v_i are unknown, and employ only a sound broadcasting and receiving mechanism to ensure the hold of (1). This is enabled by establishing an equivalence between sound frequency consensus and velocity consensus based on Doppler's effect, as we introduce next.

Suppose each robot is equipped with a sound-emitting device that can broadcast a sound signal at frequency $f_i(t) \in \mathbb{R}_+$. Depending on sound strength and physical distance, each robot can receive the sound from robots $j \in \mathcal{N}_i$, with $\mathcal{N}_i$ being the neighbor set of i. We assume there is no self-loop, i.e., $i \notin \mathcal{N}_i$. The robots then identify the frequency of the received sound as $r_{ij}(t)$. When the velocities of the vehicles are different, the frequency $r_{ij}(t)$ received by robot i may not equal to the sending frequency $f_j(t)$. Such phenomenon is characterized by the Doppler's effect, which reads

$$r_{ij} = \left(\frac{c - |v_i| \cos(\theta_{ij})}{c + |v_j| \cos(\theta_{ji})} \right) f_j \quad j \in \mathcal{N}_i \tag{2}$$

where $c \in \mathbb{R}_+$ is speed of sound in the medium; $\theta_{ij}(t)$ and $\theta_{ji}(t)$ (rad) are the angles between the receiver/send's forward velocity and the line connecting them, as demonstrated in Fig. 1[1]. The receiving frequency $r_{ij}(t)$ depends on the radial velocity of the two vehicles. For simplicity, the time indicator t is omitted from equations.

We assume robot i only has access to receiving frequencies $r_{ij}(t)$, $j \in \mathcal{N}_i$, and its own sending frequency $f_i(t)$, without any knowledge of v_i and θ_i. Furthermore, we assume the following assumption holds:

[1]While the figure is given in 2-D, the definition can be easily generalized to 3-D angles.

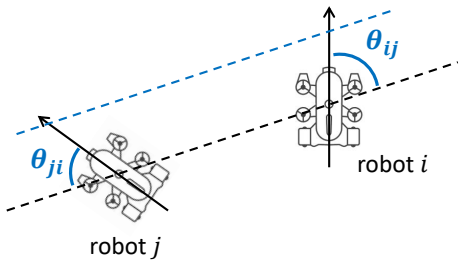

Fig. 1. Two robots that define angles θ_{ij} and θ_{ji}. The black dotted line is defined by the current positions of the two robots. The blue line is defined by the positions of the two robots after a certain time period.

Assumption 1: For all t, $i \in \{1, \ldots, m\}$, $|v_i(t)| < c$, and $f_i(t) > 0$.

Remark 2.1: Note that c is the speed of sound in the medium. For underwater applications $c = 1500m/s$ which is significantly larger than common underwater vehicles with $|v_i| < 10m/s$. For aerial applications, $c = 340m/s$ is still larger than most small-size mobile robots. For frequency, the common acoustic frequencies used in underwater application are between 5kHz-20kHz [22]. Although not analyzed in this paper, one way to ensure these conditions hold for all t is by applying thresholds to variables $v_i(t)$ and $f_i(t)$. In the extreme cases, when $|v_i| > c$ or $f_i(t) = 0$, the robots may no longer receive sounds from each other. □

Equivalence between frequency and velocity consensus.

To characterize the collective behavior of the overall multi-robot systems, we first introduce a graph $\mathbb{G}(\mathcal{V}, \mathcal{E})$ based on the neighboring relation $\mathcal{N}_i$. Here, $\mathcal{V}$ is the node set of $\mathbb{G}$ with $|\mathcal{V}| = m$ and each node represents one robot in the system; $\mathcal{E}$ is the edge set, where $(i,j) \in \mathcal{E}$ if and only if $j \in \mathcal{N}_i$. We assume the edge relation is fixed and bi-directional, i.e. $(i,j) \in \mathcal{E} \Leftrightarrow (j,i) \in \mathcal{E}$, thus $\mathbb{G}$ is fixed and undirected.

Under network $\mathbb{G}$, we use the following lemma to present the equivalence between frequency and velocity consensus of the multi-robot system.

Lemma 2.2: (Equivalence between two consensus conditions.): Suppose Assumption 1 holds. If all robots $i \in \{1, \cdots, m\}$ maintain constant velocity $v_i^\star$; broadcast constant frequency $f_i^\star$; and receive constant frequency $r_{ij}^\star$ from other robots $j \in \mathcal{N}_i$, then the following conditions are equivalent

(i) Velocity consensus among connected robots: $v_i^\star = v_j^\star$, for all $(i,j) \in \mathcal{E}$;

(ii) Frequency consensus among connected robots: $r_{ij}^\star = f_i^\star$, for all $(i,j) \in \mathcal{E}$.

Proof: The derivation of (i)→(ii) is trivial. $v_i^\star = v_j^\star$ implies $cos(\theta_{ij}) = -cos(\theta_{ji})$ (cf. Fig. 1), i.e., robot i and robot j must move towards the same direction. Thus, $v_i^\star = v_j^\star$ yields $r_{ij}^\star = f_j^\star$ from equation (2). In the following, we focus on (ii) → (i). Bringing $r_{ij}^\star = f_i^\star$ into (2), one has

$$\left(c + |v_j^\star| \cos(\theta_{ji})\right) f_i^\star = \left(c - |v_i^\star| \cos(\theta_{ij})\right) f_j^\star \tag{3a}$$

$$\left(c + |v_i^\star| \cos(\theta_{ij})\right) f_j^\star = \left(c - |v_j^\star| \cos(\theta_{ji})\right) f_i^\star \tag{3b}$$

where the first equation considers i as the receiver, and the second equation considers j as the receiver. As a consequence of (3), for any two neighboring robots,

$$\frac{c-|v_i^\star|\cos(\theta_{ij})}{c+|v_i^\star|\cos(\theta_{ij})}=\frac{c+|v_j^\star|\cos(\theta_{ji})}{c-|v_j^\star|\cos(\theta_{ji})}. \tag{4}$$

Given Assumption 1 that $|v_i|<c$, $|v_j|<c$, one has

$$|v_i^\star|\cos(\theta_{ij})=-|v_j^\star|\cos(\theta_{ji}) \tag{5}$$

To make sure the frequency consensus $r_{ij}^\star=f_i^\star$ is reached for all $(i,j)\in\mathcal{E}$, equation (5) must holds. Recall that $v_i^\star$, $v_j^\star$ and $f_j^\star$ have constant values. Thus, one can obtain θ_{ij} and θ_{ji} also being constants from (2). This, as visualized in Fig. 1, implies

$$|v_i^\star|\sin(\theta_{ij})=|v_j^\star|\sin(\theta_{ji}). \tag{6}$$

Note that (6) means that the tangent speeds of the robots are the same, so the dash lines (blue and black) defined by the two robots are parallel. Finally, bringing equations (5)-(6) together, when $|v_i^\star|\neq 0$, $i\in\{1,\cdots,m\}$ (otherwise the problem is trivial), there holds:

$$|v_i^\star|=|v_j^\star|,\qquad \theta_{ij}^\star+\theta_{ji}^\star=\pi \tag{7}$$

this further yields

$$v_i^\star=v_j^\star \tag{8}$$

This completes the proof. ■

Remark 2.3: While Lemma 2.2 introduces equivalence among neighboring agents, if the underlying network $\mathbb{G}$ is connected, (8) leads to (1). This implies the velocity consensus across the whole multi-robot system can be achieved by their frequency consensus.

III. Distributed control for 1-D velocity consensus

Designing a distributed algorithm for achieving (2) is very challenging, due to the limited information (only $f_i(t)$ and $r_{ij}(t)$) each robot can access. In this paper, we study a simplified version of problem (1), which aims to design a distributed control algorithm for the 1-D case, where all robots move over a line and $v_i\in\mathbb{R}$ is a scalar. The potential applications of this include underwater line (pipelines, fiber-optic cables, etc) following and flocking, or highway traffic speed consensus. Under 1-D condition, for all $i,j\in\{1,\cdots,m\}$, one has $\cos(\theta_{ij})=\pm 1$. We assume the robots are far away from each other and reorder their indexes sequentially depending on their relative position, as shown in Fig. 2. We also set $v_i>0$ when the robot i moves towards a lower indexed robot, and $v_i<0$ otherwise. Based on these definitions, the relative velocities used in (2) can be rewritten as

$$|v_i|\cos(\theta_{ij})=s_{ij}v_i,\qquad s_{ij}=\begin{cases}1 & \text{for}\quad i\leqslant j\\ -1 & \text{for}\quad i>j\end{cases} \tag{9}$$

Fig. 2. 1-D robot flocking.

By substituting (9) into Doppler's effect equation (2), and using the property $s_{ij}=-s_{ji}$, one has

$$r_{ij}=\left(\frac{c-s_{ij}v_i}{c-s_{ij}v_j}\right)f_j\quad j\in\mathcal{N}_i \tag{10}$$

To explain equation (10), when a former robot i moves faster than a latter robot j, $(i<j)$, the robots are further apart from each other and the received frequency r_{ij} is lower than the sending frequency f_j, and vice versa.

A. A distributed algorithm for velocity consensus.

To achieve the velocity consensus (1) based solely on comparing $r_{ij}(t)$ and $f_i(t)$, we design the following dynamics:

$$\dot{v}_i=k_1\sum_{j\in\mathcal{N}_i}(s_{ij}(r_{ij}-f_i)) \tag{11a}$$

$$\dot{f}_i=k_2\sum_{j\in\mathcal{N}_i}(r_{ij}-f_i) \tag{11b}$$

where $k_1,k_2\in\mathbb{R}_+$ are constant control gains.

Remark 3.1: (Algorithm explained.): The intuition behind dynamics (11) is to simultaneously manipulate the velocity and sending frequency of robot i in order to minimize the difference between $f_i(t)$ and $r_{ij}(t)$, $j\in\mathcal{N}_i$. Driven by this, the dynamics (11b) is straight forward since it drives $f_i(t)$ towards the average of $r_{ij}(t)$. The computation of such average does not require robot i to identify the indexes of robots $j\in\mathcal{N}_i$. The dynamics (11a) is an inverse use of Doppler's effect, which drives robot i to increase its speed towards robot j if the receiving frequency $r_{ij}(t)$ is lower than its $f_i(t)$ so that $r_{ij}(t)$ will increase. Note that the implementation of (11a) requires the identification of $s_{ij}=\pm 1$. This can be addressed (i) by the sender, through encoding the index information into the sound broadcasting process; (ii) by the receiver, through identifying the direction of the sound source; (iii) by the receiver, through a simple first order approximation of (10) that observes how $r_{ij}(t)$ changes with the change of $v_i(t)$. Since s_{ij} only takes binary values (± 1), an robust approximation can be achieved. ▫

From (11), it can be observed that the coordination among two connected robots $(i,j)\in\mathcal{E}$ is asymmetric because $s_{ij}\neq s_{ji}$. For the convenience of analyzing such relation, we introduce two graphs $\mathbb{G}_1(\mathcal{V},\mathcal{E}_1)$ and $\mathbb{G}_2(\mathcal{V},\mathcal{E}_2)$ as edge-reduced graphs of $\mathbb{G}$, such that $(i,j)\in\mathcal{E}_1$ if $(i,j)\in\mathcal{E}$ and $i<j$; $(i,j)\in\mathcal{E}_2$ if $(i,j)\in\mathcal{E}$ and $i>j$. Specifically , $\mathbb{G}_1$ takes the edges of $\mathbb{G}$ directing from lower indexed nodes to larger indexed nodes; while $\mathbb{G}_2$ takes the edges of $\mathbb{G}$ directing from larger indexed nodes to lower indexed nodes.

Assumption 2: The edge-reduced graphs $\mathbb{G}_1(\mathcal{V},\mathcal{E}_1)$ and $\mathbb{G}_2(\mathcal{V},\mathcal{E}_2)$ of $\mathbb{G}$ are both spanned by directed rooted trees.

The simplest graph $\mathbb{G}$ satisfying Assumption 2 is an undetected path graph connecting from robots 1 to m.

Theorem 3.2: (Local convergence around equilibrium points): Suppose Assumption 2 holds. Consider an equilibrium of dynamics (11) such that $\forall i \in \{1, \cdots, m\}$, $v_i^\star = v^\star$ and $f_i^\star = f^\star$. Suppose $f^\star > 0$ and $|v^\star| < c$. Then, within the neighborhood of this equilibrium, dynamics (11) is locally asymptotically convergent to the invariant set defined by $v_1 = \cdots = v_m$ and $f_1 = \cdots = f_m$.

Remark 3.3: (Local v.s. global convergence): Given dynamics (11), it is clear that any point in the consensus invariant set, i.e., $v_1 = \cdots = v_m$ and $f_1 = \cdots = f_m$ is an equilibrium of dynamics (14). Theorem 3.2 states that within the neighborhood of this invariant set, the algorithm converges asymptotically back to this set. Here, we only analyze the local stability due to the difficulty in determining the global stability of dynamics (11). Specifically, note that (i) r_{ij} is highly nonlinear. As shown in (10), f_i and v_i are coupled on the nominator and v_j appears on the denominator of the equation. (ii) the graph information embedded in s_{ij} is asymmetric among connected agents. The two reasons make it difficult to employ existing techniques such as Lyapunov stability theorem to prove global convergence.

Nevertheless, building on our results on local convergence, later in Remark 3.5, we will briefly quantify the convergence region and discuss possible ways to enlarge this region. □

B. Proof of the main theorem

Linearization: For the convenience of presentation, let

$$g_i(\cdot) = -\sum_{j\in\mathcal{N}_i}\left(s_{ij}\left(\frac{c - s_{ij}v_i}{c - s_{ij}v_j}f_j - f_i\right)\right)$$
$$h_i(\cdot) = -\sum_{j\in\mathcal{N}_i}\left(\frac{c - s_{ij}v_i}{c - s_{ij}v_j}f_j - f_i\right).$$

To analyze the local stability, we linearize the dynamics around equilibriums $v_i = v_j = v^\star$ and $f_i = f_j = f^\star$ as:

$$\dot{v}_i = -k_1\sum_{j\in\mathcal{N}_i}\left(\left.\frac{\partial g_i}{\partial v_j}\right|_{\substack{v_i=v_j=v^\star\\ f_i=f_j=f^\star}} v_j + \left.\frac{\partial g_i}{\partial f_j}\right|_{\substack{v_i=v_j=v^\star\\ f_i=f_j=f^\star}} f_j\right) \quad (12a)$$

$$\dot{f}_i = -k_2\sum_{j\in\mathcal{N}_i}\left(\left.\frac{\partial h_i}{\partial v_j}\right|_{\substack{v_i=v_j=v^\star\\ f_i=f_j=f^\star}} v_j + \left.\frac{\partial h_i}{\partial f_j}\right|_{\substack{v_i=v_j=v^\star\\ f_i=f_j=f^\star}} f_j\right) \quad (12b)$$

where, for $j \in \mathcal{N}_i$ and $j = i$, one has

$$\left.\frac{\partial g_i}{\partial v_j}\right|_{\substack{v_i=v_j=v^\star\\ f_i=f_j=f^\star}} = \begin{cases} -\frac{f^\star}{c - s_{ij}v^\star} & \text{for} \quad i \neq j \\ \sum_{k\in\mathcal{N}_i}\frac{f^\star}{c - s_{ik}v^\star} & \text{for} \quad i = j \end{cases} \quad (13a)$$

$$\left.\frac{\partial g_i}{\partial f_j}\right|_{\substack{v_i=v_j=v^\star\\ f_i=f_j=f^\star}} = \begin{cases} -s_{ij} & \text{for} \quad i \neq j \\ \sum_{k\in\mathcal{N}_i} s_{ik} & \text{for} \quad i = j \end{cases} \quad (13b)$$

$$\left.\frac{\partial h_i}{\partial v_j}\right|_{\substack{v_i=v_j=v^\star\\ f_i=f_j=f^\star}} = \begin{cases} -\frac{s_{ij}f^\star}{c - s_{ij}v^\star} & \text{for} \quad i \neq j \\ \sum_{k\in\mathcal{N}_i}\frac{s_{ik}f^\star}{c - s_{ik}v^\star} & \text{for} \quad i = j \end{cases} \quad (13c)$$

$$\left.\frac{\partial h_i}{\partial f_j}\right|_{\substack{v_i=v_j=v^\star\\ f_i=f_j=f^\star}} = \begin{cases} -1 & \text{for} \quad i \neq j \\ \sum_{k\in\mathcal{N}_i} 1 & \text{for} \quad i = j \end{cases} \quad (13d)$$

Following equation (13), we define Laplacian-like matrices $L_F, L_S, L_{SF}, L_{\mathbb{G}} \in \mathbb{R}^{m\times m}$ whose entries are $L_F[i,j] = \frac{\partial g_i}{\partial v_j}$, $L_S[i,j] = \frac{\partial g_i}{\partial f_j}$, $L_{SF}[i,j] = \frac{\partial h_i}{\partial v_j}$, and $L_{\mathbb{G}}[i,j] = \frac{\partial h_i}{\partial f_j}$. Here, $L_{\mathbb{G}}$ is the exact Laplacian matrix of $\mathbb{G}$, the other matrices are called Laplacian-like because they are re-weighted variants of $L_{\mathbb{G}}$ still preserving the property of row sum being zero. Based on the defined matrices, we can rewrite the linearized dynamics (12) into the following compact form:

$$\dot{\boldsymbol{v}} = -k_1(L_F\boldsymbol{v} + L_S\boldsymbol{f}) \quad (14a)$$
$$\dot{\boldsymbol{f}} = -k_2(L_{SF}\boldsymbol{v} + L_{\mathbb{G}}\boldsymbol{f}) \quad (14b)$$

where $\boldsymbol{v} = \text{col}\{v_1(t), \cdots v_m(t)\} \in \mathbb{R}^m$, and $\boldsymbol{f} = \text{col}\{f_1(t), \cdots f_m(t)\} \in \mathbb{R}^m$.

Transformation: For the convenience of studying the convergence of (14), recall the two edge-reduced graphs $\mathbb{G}_1(\mathcal{V}, \mathcal{E}_1)$ and $\mathbb{G}_2(\mathcal{V}, \mathcal{E}_2)$ defined above Assumption 2. Let $L_{\mathbb{G}_1}$ and $L_{\mathbb{G}_2}$ be the Laplacian matrices corresponding to the two graphs. By definition, $L_{\mathbb{G}_1}$ is an upper triangular matrix, and $L_{\mathbb{G}_2}$ is a lower triangular matrix. Furthermore, based on (13) and the definitions of $L_F, L_S, L_{SF}, L_{\mathbb{G}}$, one has

$$L_{\mathbb{G}} + L_S = 2L_{\mathbb{G}_1}, \qquad L_{\mathbb{G}} - L_S = 2L_{\mathbb{G}_2}, \quad (15a)$$
$$L_F + L_{SF} = 2\beta_1 L_{\mathbb{G}_1}, \quad L_F - L_{SF} = 2\beta_2 L_{\mathbb{G}_2}. \quad (15b)$$

where $\beta_1 = \frac{f^\star}{c - v^\star}$, $\beta_2 = \frac{f^\star}{c + v^\star}$. Here (15b) is derived from (13a,c) where $s_{ij} = 1$ for $i < j$ and $s_{ij} = -1$ for $i > j$.

To continue, we show the local convergence of (14) by studying the eigenvalues of

$$Q = \begin{bmatrix} k_1 L_F & k_1 L_S \\ k_2 L_{SF} & k_2 L_{\mathbb{G}} \end{bmatrix}.$$

Define the following transformation matrices

$$T = \begin{bmatrix} k_1 I_m & -k_1 I_m \\ k_2 I_m & k_2 I_m \end{bmatrix}, \quad T^{-1} = \frac{1}{2k_1k_2}\begin{bmatrix} k_2 I_m & k_1 I_m \\ -k_2 I_m & k_1 I_m \end{bmatrix}$$

Then based on (15), the similarity transformation of Q yields:

$$T^{-1}QT = \begin{bmatrix} (k_2 + k_1\beta_1)L_{\mathbb{G}_1} & (k_2 - k_1\beta_1)L_{\mathbb{G}_1} \\ (k_2 - k_1\beta_2)L_{\mathbb{G}_2} & (k_2 + k_1\beta_2)L_{\mathbb{G}_2} \end{bmatrix} \quad (16)$$

Lemma 3.4: Given Assumption 2, suppose $f^\star > 0$ and $|v^\star| < c$. The following statements hold

(i) $\lambda = 0$ is the eigenvalue of $T^{-1}QT$ with geometric multiplicity equals to two. The corresponding eigenvectors can be chosen as $\text{col}\{\mathbf{1}_m, \mathbf{0}_m\}$ and $\text{col}\{\mathbf{0}_m, \mathbf{1}_m\}$.

(ii) Except for $\lambda = 0$, all other eigenvalues of $T^{-1}QT$ have positive real parts.

The proof of this lemma is given in appendix (Arxiv).

Convergence: We make use of Lemma 3.4 to prove the convergence of dynamics (14). Define a new state variable $\boldsymbol{x} \in \mathbb{R}^{2m}$ such that $\begin{bmatrix}\boldsymbol{v}\\ \boldsymbol{f}\end{bmatrix} = T\boldsymbol{x}$. Then (14) is equivalent to

$$\dot{\boldsymbol{x}} = -T^{-1}QT\boldsymbol{x}. \quad (17)$$

where $T^{-1}QT$ is defined in (16). From Lemma 3.4, and the LaSalle's invariance principle [23] for linear systems, we know $\boldsymbol{x}$ converges asymptotically to $\boldsymbol{x}^\dagger$, which lies in

the invariant set spanned by the eigenvectors of $T^{-1}QT$ corresponding to its zero eigenvalues, i.e.,

$$\boldsymbol{x}^{\dagger} \in \text{image}\left(\begin{bmatrix}\mathbf{1}_m\\ \mathbf{0}_m\end{bmatrix}\right) \bigcup \text{image}\left(\begin{bmatrix}\mathbf{0}_m\\ \mathbf{1}_m\end{bmatrix}\right).$$

Consequently, the $\boldsymbol{v}$ and $\boldsymbol{f}$ in update (14) converge to

$$\begin{aligned}\begin{bmatrix}\boldsymbol{v}^{\dagger}\\ \boldsymbol{f}^{\dagger}\end{bmatrix} &\in \text{image}\left(T\begin{bmatrix}\mathbf{1}_m\\ \mathbf{0}_m\end{bmatrix}\right) \bigcup \text{image}\left(T\begin{bmatrix}\mathbf{0}_m\\ \mathbf{1}_m\end{bmatrix}\right)\\ &= \text{image}\left(\begin{bmatrix}\mathbf{1}_m\\ \mathbf{0}_m\end{bmatrix}\right) \bigcup \text{image}\left(\begin{bmatrix}\mathbf{0}_m\\ \mathbf{1}_m\end{bmatrix}\right), \qquad (18)\end{aligned}$$

where the subspace is invariant under transformation matrix T. Clearly, (18) indicates the consensus condition $v_1 = \cdots = v_m$ and $f_1 = \cdots = f_m$. This completes the proof. ■

Remark 3.5: (Local convergence and convergence region.): Theorem 3.2 proves only the *local* convergence of (11). The convergence region is impacted by the approximation error of linearization (12). To quantify this, subtract the linearized dynamics (12) and the original dynamics (11). The approximation error on f_j is proportional to $|\frac{v_j - v_i}{c - s_{ij} v_j}|$. To reduce this term, one can assume that $\frac{|v_i|}{c}$ is sufficiently small for all robots. The approximation error on v_j is proportional to $|\frac{f_j - f^{\star}}{c}|$. To reduce this term, a possible approach is to set $\frac{k_1}{k_2}$ being sufficiently small. Then dynamics (11) forms a two-time scale system [24], with (11b) being the fast system and (11a) being the slow system. Consequently, when the algorithm starts, dynamics (11b) will converge quickly to a neighborhood of frequency consensus, where $|\frac{f_j - f^{\star}}{c}|$ is small enough to make sure the linearized system closely approximates the nonlinear dynamics. To conclude, assuming small $\frac{|v_i|}{c}$ and $\frac{k_1}{k_2}$ is beneficial for expanding the local convergence to a larger region. As will be validated in the simulation section, with $\frac{|v_i(0)|}{c} < 0.01$ and $\frac{k_1}{k_2} = 0.01$, nonlinear dynamics (11) converge asymptotically to consensus condition even if the initial states are far away from any equilibrium.

IV. Simulations Results

In this section, we apply the proposed distributed algorithm by *Matlab Simulink* to achieve the velocity consensus of multi-robot systems in 1-D environments. In the simulation, we conduct tests with 10 robots and the dynamics of the algorithm in the simulation is given by equation (11) as a continuous-time model. The corresponding communication topology is characterized by an undirected Erdős–Rónyi graph, where the probability of any two nodes in the graph being connected is 60%. We verify that the obtained graph is connected which satisfies Assumption 1.

Following Remark 3.5, the parameters k_1 and k_2 of the algorithm in the simulation are selected as:

$$k_1 = 0.1, k_2 = 10 \qquad (19)$$

so that $\frac{k_1}{k_2} = 0.01$ (cf. Remark 3.5).

We validate the effectiveness of the proposed algorithm. The initial conditions of frequencies $f_i(0)$ (Hz) and velocities $v_i(0)$ (m/s) of each robot in the simulation is given as:

$$f_i(0) \sim U(4500, 7500), \quad v_i(0) \sim U(1, 9), \forall i \in \mathcal{V}. \qquad (20)$$

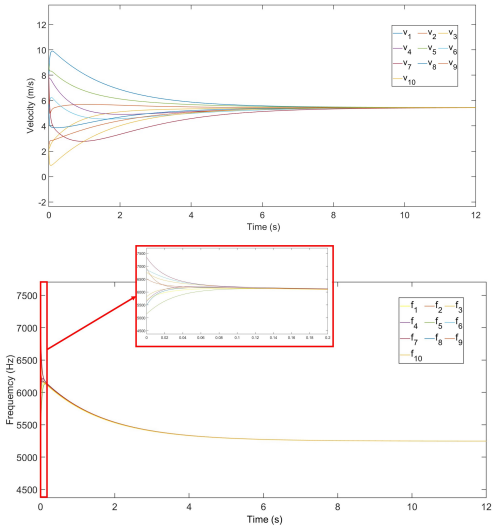

Fig. 3. Results of the consensus algorithm without noise.

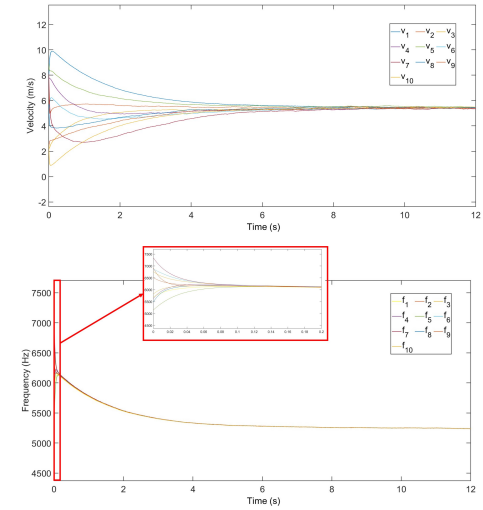

Fig. 4. Results of the consensus algorithm when noise $\omega_{ij} \sim N(0, 50^2)$.

where $U(a, b)$ represents uniform distribution, and a,b define the lower and upper bounds. Here, $c = 1500m/s$ and we have $\frac{|v_i(0)|}{c} < 0.01$. To further validate the performances of the proposed algorithm, we consider the situation when the received frequency r_{ij} of each robot is subject to a noise $\omega_{ij}(t)$. All $\omega_{ij}(t)$ are assumed to be discrete Gaussian white noise with zero mean $\mathbb{E}(\omega_{ij}) = 0$. Then the dynamics of the system (c.f. equation (11)) becomes

$$\dot{v}_i = k_1 \sum_{j \in \mathcal{N}_i} (s_{ij}(r_{ij} + \omega_{ij} - f_i)) \qquad (21a)$$

$$\dot{f}_i = k_2 \sum_{j \in \mathcal{N}_i} (r_{ij} + \omega_{ij} - f_i) \qquad (21b)$$

Fig. 3 illustrates the dynamics of the system when the noise of received frequency is equal to 0, i.e., no noise. The result shows that the velocity consensus and frequency consensus are perfectly achieved based on the proposed algorithm. As shown in fig. 4, when noise $\omega_{ij} \sim N(0, 50^2)$, the velocities robots will converge to the steady state with small variations. We quantify the variation by $R = \max_i(v_i^s) - \min_j(v_j^s)$

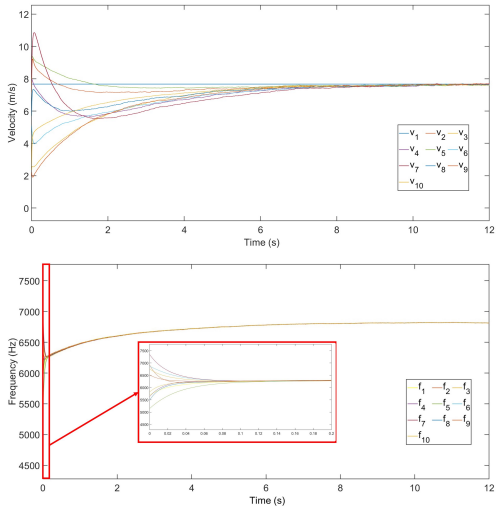

Fig. 5. Results of the leader-follower consensus algorithm when noise $\omega_{ij} \sim N(0, 50^2)$.

with v_i^s being the robots' velocities in steady states. We can see all the velocities reaches steady states from 9.32 second, and range $R = 0.04 \quad m/s$, which shows the effectiveness of the algorithm when measurements are subject to noises.

Finally, we extend to a leader-follower scenario to test the performance of the algorithm. Here we assign robot 1 as the leader of the system. Then the dynamic model of the system becomes:

$$\dot{v}_i = \begin{cases} 0 & \text{for} \quad i = 1 \\ k_1 \sum_{j \in \mathcal{N}_i} (s_{ij}(r_{ij} + \omega_{ij} - f_i)) & \text{for} \quad i \neq 1 \end{cases} \tag{22a}$$

$$\dot{f}_i = k_2 \sum_{j \in \mathcal{N}_i} (r_{ij} + \omega_{ij} - f_i) \tag{22b}$$

The initial conditions of frequencies $f_i(0)$ and velocities $v_i(0)$ of each robot is given as equation (20), and the measurement noise $\omega_{ij} \sim N(0, 50^2)$. As shown in Fig. 5, robots' velocities will converge towards the leader's velocity with variations $R = 0.04 m/s$.

V. Conclusions and Future Work

In this paper, we have introduced a new distributed algorithm for multi-robot systems to achieve the velocity consensus under denied environments based on the Doppler effect. The proposed algorithm is fully distributed which only uses its local information and is robust to the time-varying communication graph. Moreover, the algorithm only requires measurements of sound frequency as a medium for multi-robot coordination, instead of depending on any direct or relative measurements of the velocity. Thus, our algorithm is beneficial for solving the issue of interference and scalability in large-scale networks. Future works include global convergence analysis and will extend to 2-D and 3-D cases, which are applicable to more complicated application scenarios. In addition, we will test the proposed algorithm under real robot platforms.

References

[1] P. Zhu and W. Ren, "Fully distributed joint localization and target tracking with mobile robot networks," *IEEE Transactions on Control Systems Technology*, vol. 29, no. 4, pp. 1519–1532, 2021.

[2] X. Wang, J. Zhou, S. Mou, and M. J. Corless, "A distributed algorithm for least squares solutions," *IEEE Transactions on Automatic Control*, vol. 64, no. 10, pp. 4217–4222, 2019.

[3] R. Olfati-Saber, "Distributed kalman filtering for sensor networks," in *2007 46th IEEE Conference on Decision and Control*, 2007, pp. 5492–5498.

[4] H. Cai and J. Huang, "The leader-following attitude control of multiple rigid spacecraft systems," *Automatica*, vol. 50, no. 4, pp. 1109–1115, 2014.

[5] X. Wang, S. Mou, and S. Sundaram, "Resilience for distributed consensus with constraints," *arXiv preprint arXiv:2206.05662*, 2022.

[6] J. Wu, S. Yuan, S. Ji, G. Zhou, Y. Wang, and Z. Wang, "Multi-agent system design and evaluation for collaborative wireless sensor network in large structure health monitoring," *Expert Systems with Applications*, vol. 37, no. 3, pp. 2028–2036, 2010.

[7] X. Wang, S. Mou, and S. Sundaram, "A resilient convex combination for consensus-based distributed algorithms," *Numerical Algebra, Control & Optimization*, vol. 9, no. 3, pp. 269–281, 2019.

[8] C. Yan and H. Fang, "A new encounter between leader–follower tracking and observer-based control: Towards enhancing robustness against disturbances," *Systems & Control Letters*, vol. 129, pp. 1–9, 2019.

[9] X. Wang, S. Mou, and B. D. Anderson, "Consensus-based distributed optimization enhanced by integral feedback," *IEEE Transactions on Automatic Control*, vol. 68, no. 3, pp. 1894–1901, 2022.

[10] Z. Zhou, J. Liu, and J. Yu, "A survey of underwater multi-robot systems," *IEEE/CAA Journal of Automatica Sinica*, vol. 9, no. 1, pp. 1–18, 2022.

[11] W. Ren and N. Sorensen, "Distributed coordination architecture for multi-robot formation control," *Robotics and Autonomous Systems*, vol. 56, no. 4, pp. 324–333, 2008.

[12] X. Chen, M.-A. Belabbas, and T. Başar, "Controllability of formations over directed time-varying graphs," *IEEE Transactions on Control of Network Systems*, vol. 4, no. 3, pp. 407–416, 2015.

[13] F. Bullo, *Lectures on network systems*. Kindle Direct Publishing Santa Barbara, CA, 2019, vol. 1.

[14] E. Montijano, E. Cristofalo, D. Zhou, M. Schwager, and C. Saguees, "Vision-based distributed formation control without an external positioning system," *IEEE Transactions on Robotics*, vol. 32, no. 2, pp. 339–351, 2016.

[15] J. Xu, "Underwater wireless optical communication: why, what, and how?" *Chin. Opt. Lett.*, vol. 17, no. 10, p. 100007, Oct 2019.

[16] Y. Zhou, W. Wang, H. Zhang, X. Zheng, L. Li, C. Wang, G. Xu, and G. Xie, "Underwater robot coordination using a bio-inspired electrocommunication system," *Bioinspiration and Biomimetics*, vol. 17, no. 5, p. 056005, jul 2022.

[17] C. Chevallereau, M.-R. Benachenhou, V. Lebastard, and F. Boyer, "Electric sensor-based control of underwater robot groups," *IEEE Transactions on Robotics*, vol. 30, no. 3, pp. 604–618, 2014.

[18] G. Vasiljević, T. Petrović, B. Arbanas, and S. Bogdan, "Dynamic median consensus for marine multi-robot systems using acoustic communication," *IEEE Robotics and Automation Letters*, vol. 5, no. 4, pp. 5299–5306, 2020.

[19] I. F. Akyildiz, P. Wang, and Z. Sun, "Realizing underwater communication through magnetic induction," *IEEE Communications Magazine*, vol. 53, no. 11, pp. 42–48, 2015.

[20] P. Zhang, J. Gu, E. E. Milios, and P. Huynh, "Navigation with imu/gps/digital compass with unscented kalman filter," in *IEEE International Conference Mechatronics and Automation, 2005*, vol. 3. IEEE, 2005, pp. 1497–1502.

[21] M. B. Guldogan, "Consensus bernoulli filter for distributed detection and tracking using multi-static doppler shifts," *IEEE Signal Processing Letters*, vol. 21, no. 6, pp. 672–676, 2014.

[22] R. P. Hodges, *Underwater acoustics: Analysis, design and performance of sonar*. John Wiley & Sons, 2011.

[23] J. P. La Salle, "An invariance principle in the theory of stability," Tech. Rep., 1966.

[24] H.-D. Chiang and L. F. C. Alberto, *Stability regions of two-time-scale continuous dynamical systems*. Cambridge University Press, 2015, p. 287–321.